Original paper

Chromium- and nickel-rich micas and associated minerals in listvenite from the Muránska Zdychava, Slovakia: products of hydrothermal metasomatic transformation of ultrabasic rock

Štefan FERENC[1,*], Pavel UHER[2], Ján SPIŠIAK[1], Viera ŠIMONOVÁ[1]

[1] *Department of Geography and Geology, Faculty of Natural Sciences, Matej Bel University, Tajovského 40, 974 01 Banská Bystrica, Slovak Republic; stefan.ferenc@umb.sk*

[2] *Department of Mineralogy and Petrology, Faculty of Natural Sciences, Comenius University, Ilkovičova 6, 842 15 Bratislava, Slovak Republic*

**Corresponding author*

The Cr–Ni-rich micas, Ni–Co sulphide phases and associated minerals occur in a small body of listvenite, an extensively altered serpentinite, in Lower Palaeozoic paragneisses near Muránska Zdychava village in Slovenské Rudohorie Mts. (Veporic Superunit, central Slovakia). The main rock-forming minerals of the listvenite are magnesite, dolomite and a serpentine-group mineral, less frequently calcite, quartz and talc. Accessory minerals of the listvenite include Cr–Ni-rich micas, chromite, and Ni–Co–Fe–(Cu–Pb) sulphide minerals (pyrite, pyrrhotite, pentlandite, millerite, polydymite, violarite, siegenite, gersdorffite, cobaltite, chalcopyrite and galena). The micas from the Muránska Zdychava listvenite (Cr–Ni-rich illite to muscovite and Ni-dominant trioctahedral mica) contain the highest Ni concentrations ever reported in the mica-group minerals (up to 22.8 wt. % NiO or 1.46 *apfu* Ni). The Cr concentrations are also relatively high (up to 11.0 wt. % Cr_2O_3 or 0.64 *apfu*). Compositional variations in both Cr–Ni-rich mica minerals are characterized by the negative Cr vs. Ni correlation that indicates a dominant role of $2^{O}M^{3+} + {}^{O}\square = 3^{O}M^{2+}$ and ${}^{O}M^{3+} + {}^{T}Al = {}^{O}M^{2+} + {}^{T}Si$ substitution mechanisms. Chromite is dominated by Fe^{2+} (0.82–0.90 *apfu*) and Cr (1.38–1.79 *apfu*).

The listvenite contains ~0.3 wt. % Cr_2O_3 and ~0.2 wt. % NiO. It represents a good example of multistage transformation of an ultrabasic protolith, reflecting variable alteration. The incipient alteration leads to relatively high SiO_2, MgO, and Cr_2O_3 contents, the latter two typical of ultrabasic rocks. The more advanced alteration stage shows lower SiO_2, but higher content of volatiles (*c.* 35 wt. % of LOI) bound in carbonates and hydrated silicate minerals. Based on geochemical and mineralogical characteristics, the studied listvenite body originated during three principal evolutionary stages: (1) peridotite stage, (2) serpentinization stage, and (3) hydrothermal–metasomatic stage (listvenitization). The listvenite origin was probably connected with Alpine (Late Cretaceous) late-orogenic uplift of the Veporic Superunit crystalline basement and retrograde metamorphism; we assume P–T conditions of the final listvenite stage at ~200 MPa and up to 350 °C. The NE–SW and NW–SE trending fault structures played a key role during the process of listvenitization as they channelized the CO_2-rich fluids that transformed the serpentinized peridotite into the carbonate–quartz listvenite.

Keywords: Cr–Ni mineralization, listvenite, Cr–Ni-rich mica, Ni–Co sulphide minerals, Veporic Superunit, Western Carpathians
Received: 14 March, 2016; accepted: 26 August, 2016; handling editor: F. Laufek

1. Introduction

Term listvenite (listwanite) is generally used for metasomatic rocks, products of strong transformation (carbonatization, silicification) of primary ultrabasic rocks in ophiolite complexes of various ages (e.g., Sazonov 1975; Hansen et al. 2005; Akbulut et al. 2006). Listvenitization of the ultrabasic rocks belongs to mesothermal processes, where the study of fluid inclusions in minerals and other data indicate temperatures of ~290 to 340 °C and pressures of ~100 to 300 MPa (Halls and Zhao 1995; Plissart et al. 2009; Bagherzadeh et al. 2013). They are commonly connected with gold mineralization or deposits (Dinel et al. 2008; Buckman and Ashley 2010; García et al. 2015 and references therein), whereas massive, tectonically less affected listvenites could be used as gemstones or decorative stones (Simic et al. 2013).

Small listvenite bodies have been described also in ultrabasic rocks of the Western Carpathians, Slovakia. They occur in Palaeozoic (pre-Carboniferous) metamorphic rocks near Jasenie, Nízke Tatry Mts. (Tatric Superunit), Muránska Dlhá Lúka, Slovenské Rudohorie Mts. (Veporic Superunit), in North-Gemeric structural zone (Dobšiná, Mlynky, Rudňany, Veľký Folkmár, Košická Belá, Bukovec, Breznička and other localities), and in anchimetamorphic Mesozoic ultramafic rocks near Bôrka in Slovenské Rudohorie Mts., Meliatic Unit (Ivan 1984, 1985; Hovorka et al. 1985).

In this paper, we characterize unusual mineralization in the listvenite body near Muránska Zdychava village

in the Veporic Superunit, central Slovakia. The carbonate–quartz listvenite contains peculiar mineralization including unique Cr–Ni-rich micas (with the highest Ni content in mica-group minerals worldwide), chromite and various Ni–Co–Fe sulphides. The preliminary results, including the mica compositions, were published previously (Uher et al. 2013); however, our contribution deals with a detailed mineral description of the whole association, the rock geochemistry and possible listvenite genesis.

2. Location and regional geology

The studied mineralization occurs in ~10 m large outcrop of listvenitized ultrabasic rocks in close vicinity of the abandoned Horal's gallery in the Rypalová Valley near Muránska Zdychava village (geographic coordinates: 48°45'24" N; 20°08'01" E), situated *c*. 8 km NNE of Revúca (Slovenské Rudohorie Mts, Central Slovakia).

The occurrence belongs to the Veporic Superunit of the Western Carpathians. The Western Carpathians represent a complex Alpine mountain belt, a part of the Alpine–Carpathian–Balkan Orogen, which resulted from a multi-stage Mesozoic to recent collision between Europe and Africa. The Western Carpathians consist of several nappe superunits, generally with northern vergency. Some superunits (Tatric, Veporic and Gemeric) include tectonic remnants of Early Palaeozoic metamorphic and magmatic basement complexes formed during the Variscan Orogeny, whereby the Veporic Superunit is sandwiched in between the underlying Tatric and overlying Gemeric superunits (e.g., Plašienka et al. 1997 and references therein).

The studied locality belongs to the Kohút Zone of the Veporic Superunit (Fig. 1). It features an allochthonous lithological sequence of Palaeozoic (pre-Carboniferous) rocks, overprinted to micaschists, paragneisses, migmatites, orthogneisses, locally with small occurrences of amphibolites, amphibolitic gneisses and rarely also ultrabasic bodies. This complex is intruded by Variscan (mainly Carboniferous) biotite tonalites, granodiorites to granites (e.g., Klinec 1976; Bezák 1982; Vass et al. 1988; Bezák et al. 1999; Hraško et al. 2005 and references therein). The listvenite body near Muránska Zdychava occurs in non-continuous NE–SW trending zone of amphibolites and small ultrabasic bodies, enclosed in garnet-bearing, muscovite–biotite micaschists to paragneisses with distinct mylonitic (phyllonitic) overprint. The listvenite alteration is restricted to ultrabasic members; basic metamorphic rocks (amphibolites and amphibolitic gneisses) were not overprinted. Geological position of the listvenite body near Muránska Zdychava (Fig. 1) indicates pre-Carboniferous age of primary magmatic ultrabasic (peridotite?) protolith.

3. Methods

Polished thin sections of listvenite were studied under polarizing optical microscope (Nikon Eclipse LV 100 POL, Matej Bel University, Banská Bystrica) in transmitted and reflected light. Chemical composition of minerals was determined by the CAMECA SX100 electron microprobe in WDS mode (State Geological Institute of Dionýz Štúr, Bratislava). Acceleration voltage of 15 kV and probe current of 20 nA for chromite, silicate and carbonate minerals, 15 kV and 10 nA for micas, and 25 kV and 10 nA for sulphide minerals were used during the electron-microprobe measurements. The following standards and spectral lines were used: wollastonite (Si K_α, Ca K_α), TiO_2 (Ti K_α), Al_2O_3 (Al K_α), native V (V K_α), native Cr (Cr K_α), fayalite (Fe K_α), rhodonite (Mn K_α), willemite and ZnS (Zn K_α), forsterite (Mg K_α), $SrTiO_3$ (Sr K_α), pyrite (Fe Kα, S K_α), native Cu (Cu K_α), native Au (Au L_α), native Ni (Ni K_α), native Co (Co K_α), GaAs (As L_α), InSb (Sb L_β), Bi_2Se_3 (Se L_β), and PbS (Pb M_α). The beam diameter of 2 to 20 μm was used with respect to the size and character of measured mineral. Detection limits for measured elements attained 0.02 to 0.1 wt. %, depending on concentration. The raw measurements were corrected by the PAP procedure (Pouchou and Pichoir 1985).

Whole-rock chemical composition of listvenite was analysed in the ACME Analytical Laboratories Ltd., Vancouver, Canada (*http://www.acmelab.com*). Samples were dissolved in Aqua Regia (AQ200). The major-element oxides were determined by the Inductively Coupled Plasma–Optical Emission Spectrometry (ICP-OES; LF300), trace elements Inductively Coupled Plasma–Mass Spectrometry (ICP-MS; LF100, LF100-EXT) analyses; C and S have been determined by the LECO induction furnace (TC003). The loss on ignition (LOI) was determined by sample annealing at 1000 °C during 2 hours.

4. Results

4.1. Zoning of the listvenite body

The listvenite outcrop shows mineral zoning and following principal petrographic types (differing

⇨

Fig. 1a – Simplified geological sketch of central part of the Slovenské Rudohorie Mts. (Slavkay et al. 2004, adapted) with the listvenite occurrence also marked. **b** – Detailed geological map of the Muránska Zdychava listvenite body and surrounding area (according to Hraško et al. 2005).

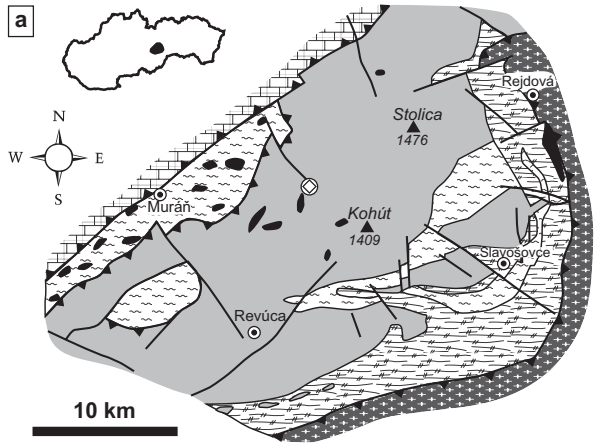

Silicicum Unit: limestones, dolomites (Triassic to Jurassic)

Gemericum Unit: clastic sediments, limestones, magnesites, lydites, phyllites and basic volcanic rocks (Devonian–Permian)

Veporicum Unit

Revúca Group: metamorphosed and unmetamorphosed clastic sedimentary rocks, volcanic rocks (Upper Paleozoic)

Phyllites, mica schists, ortho- and paragneisses (Lower Palaeozoic?)

Metabasites and ultrabasic rocks (Lower Palaeozoic?)

Undifferentiated granitoids, locally migmatitised (Carboniferous)

Thrust planes

Faults

Listvenite occurrence

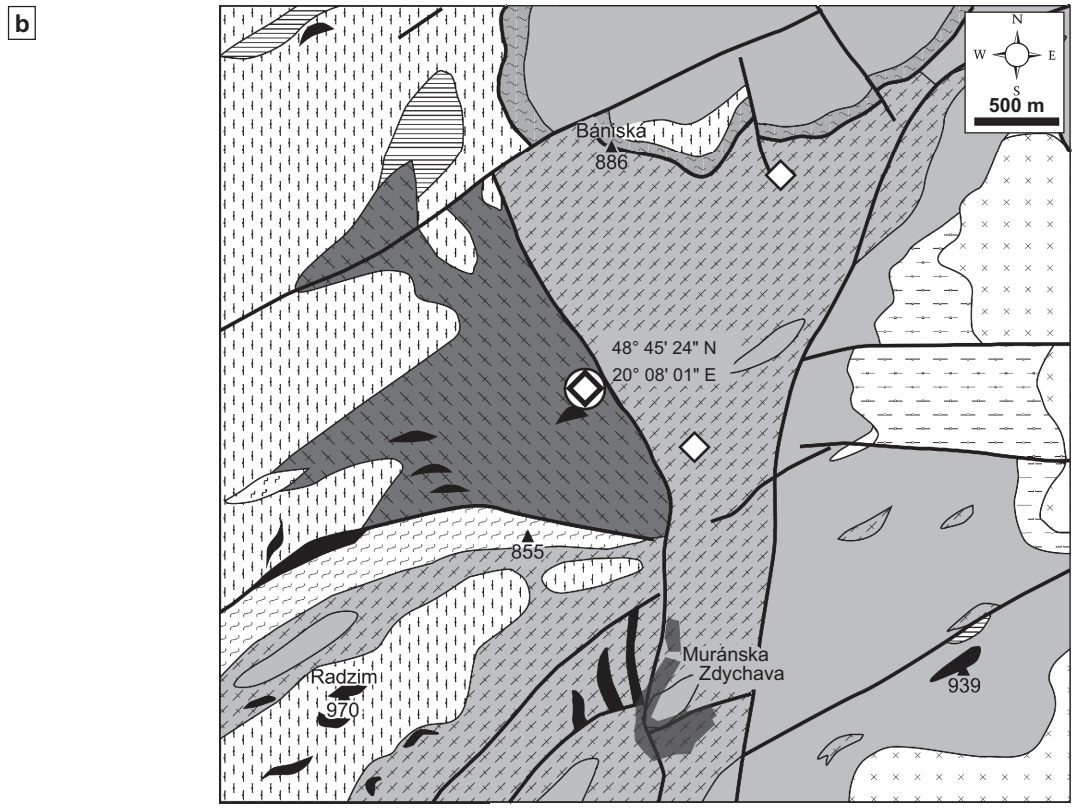

Early Palaeozoic?

Hydrothermally altered diaphtorites and phyllonites

Garnet–chlorite–muscovite schists

Biotite paragneisses, locally migmatitised

Muscovite–biotite paragneisses, locally diaphtorised

Migmatites and migmatitised gneisses

Blastoporphyric orthogneisses

Feldspar orthogneisses (Muráň Type), migmatites

Amphibolites, amphibolitic gneisses

Carboniferous

Porphyritic, biotite granites, granodiorites (Kohút Type)

Granitoids with orthogneiss bodies

Tectonic structures

Listvenite occurrence

Alpine Fe carbonate and quartz–sulphidic mineralization occurrences

mainly in the carbonate contents) in a ~10 m profile from east to west:

1) *L1 type* is relatively compact listvenite with massive structure and greyish green to pale green colour with irregular deep green domains. Locally the rock is cut by veinlets (up to 5 mm thick) of coarse- grained white calcite and yellowish fine- grained dolomite.
2) *L2 type* corresponds to yellowish-green listvenite similar to L1 type, but with stronger dolomitization.
3) *L3 type* represents grey listvenite with greenish tint and yellowish irregular veinlets/aggregates of dolomite. The rock displays slight metamorphic foliation.

4.2. Listvenite mineralogy

4.2.1. Main rock-forming minerals

The rock-forming minerals of the all three listvenite types are mainly magnesite, dolomite and serpentine-group minerals, less frequently calcite, quartz, talc, and Cr–Ni-rich members of the mica group.

Magnesite is the most common mineral of the listvenite, especially in the L1 and L2 types. On the basis of textural relationships and chemical composition, magnesite occurs in two generations. Magnesite I forms relatively coarse-grained aggregates; the size of individual grains attains 0.5 mm (Fig. 2a–b). Younger magnesite II fills veinlets (up to 0.1 mm thick) in magnesite I aggregates (Fig. 2b). Magnesite II shows higher concentration of Mg and lower Fe content compared to magnesite I (Tab. 1, Fig. 3).

Dolomite also forms two compositional types: dolomite I is slightly depleted in Mg/(Mg + Ca) (0.38–0.40), whereas dolomite II shows higher Mg/(Mg + Ca) ratio (0.47–0.48; Tab. 1, Fig. 3). Both dolomite types were probably cogenetic (Fig. 2a) and their irregular aggregates and veinlets cut the magnesite I and II (Fig. 2b).

Calcite is the youngest carbonate mineral; it forms irregular crack-fillings (≤ 5 mm thick) in magnesite I and II, dolomite I and II, Cr–Ni-rich micas and quartz. Chemical composition of the calcite is close to the ideal formula.

Quartz forms irregular aggregates, up to 0.2 mm across, or narrow veinlets in magnesite I and II (Fig. 2a–b). However, it is older than dolomite and Cr–Ni-rich micas (Fig. 2c).

Minerals of the *serpentine group* are common in all listvenite types, especially in the L3, where they locally make up a dominant part of the rock. The serpentine-group minerals (most probably antigorite) form aggregates of lamellar crystals, 50 to 100 μm in size or independent crystals in magnesite. They overgrew aggregates of magnesite I and talc (Fig. 2d). Chemical composition of the serpentine minerals (Tab. 2) shows a distinct enrichment in Fe (~7 wt. % FeO; ~0.27 *apfu*), relatively low Al content (0.6 to 1.3 wt. % Al_2O_3; 0.03–0.08 apfu), as well as elevated concentrations of Cr (0.3 to 0.9 wt. % Cr_2O_3; 0.01–0.03 *apfu*) and Ni (~0.1 wt. % NiO; ~0.005 *apfu*).

Talc forms irregular aggregates (up to 0.1 mm) in association with the serpentine-group minerals (Fig. 2d). Composition of talc (Tab. 2) shows slightly increased content of Fe (~2.4 wt. % FeO; 0.26 *apfu*) with a negligible admixture of Cr (~0.1 wt. % Cr_2O_3; 0.009 *apfu*) and Ni (~0.2 wt. % NiO; 0.025 *apfu*).

Tab. 1 Representative compositions of magnesite and dolomite from the Muránska Zdychava listvenite

wt. %									
Anal. #	MgO	CaO	FeO	MnO	SrO	Total	Mineral		
1	42.16	0.32	8.99	0.60	0.01	52.08	magnesite I		
2	42.88	0.18	9.89	0.33	0.00	53.28	magnesite I		
3	42.62	0.43	8.95	0.59	0.00	52.59	magnesite I		
4	45.08	0.12	5.07	1.24	0.00	51.50	magnesite II		
5	46.75	0.36	3.83	0.01	0.04	50.99	magnesite II		
6	45.16	0.35	6.05	0.27	0.00	51.83	magnesite II		
7	45.70	0.49	4.53	0.02	0.00	50.75	magnesite II		
8	45.27	0.66	4.82	0.04	0.00	50.80	magnesite II		
9	15.73	32.81	3.90	0.08	0.04	52.56	dolomite I		
10	14.46	32.80	5.34	0.17	0.03	52.79	dolomite I		
11	14.49	32.77	5.03	0.12	0.05	52.45	dolomite I		
12	18.87	28.72	4.40	0.16	0.07	52.22	dolomite II		
13	18.79	29.09	4.66	0.16	0.05	52.75	dolomite II		
at. %									
Anal. #	Mg	Ca	Fe	Mn	Sr	O	Mineral	Mg/(Mg+Ca)	Fe/(Mg+Fe)
1	44.11	0.24	5.28	0.35	0.00	50.01	Mgs I	0.995	0.893
2	43.98	0.14	5.69	0.19	0.00	50.01	Mgs I	0.997	0.885
3	44.13	0.32	5.20	0.35	0.00	50.01	Mgs I	0.993	0.895
4	46.27	0.09	2.92	0.72	0.00	50.01	Mgs II	0.998	0.941
5	47.52	0.27	2.18	0.01	0.01	50.01	Mgs II	0.994	0.956
6	46.12	0.25	3.47	0.16	0.00	50.01	Mgs II	0.995	0.930
7	47.00	0.36	2.62	0.01	0.00	50.01	Mgs II	0.992	0.947
8	46.69	0.49	2.79	0.02	0.00	50.01	Mgs II	0.990	0.944
9	18.92	28.37	2.63	0.06	0.02	50.00	Dol I	0.400	0.878
10	17.57	28.66	3.64	0.11	0.01	50.00	Dol I	0.380	0.828
11	17.69	28.76	3.45	0.08	0.02	50.00	Dol I	0.381	0.837
12	22.41	24.51	2.93	0.11	0.03	50.00	Dol II	0.478	0.884
13	22.14	24.64	3.08	0.10	0.02	50.00	Dol II	0.473	0.878

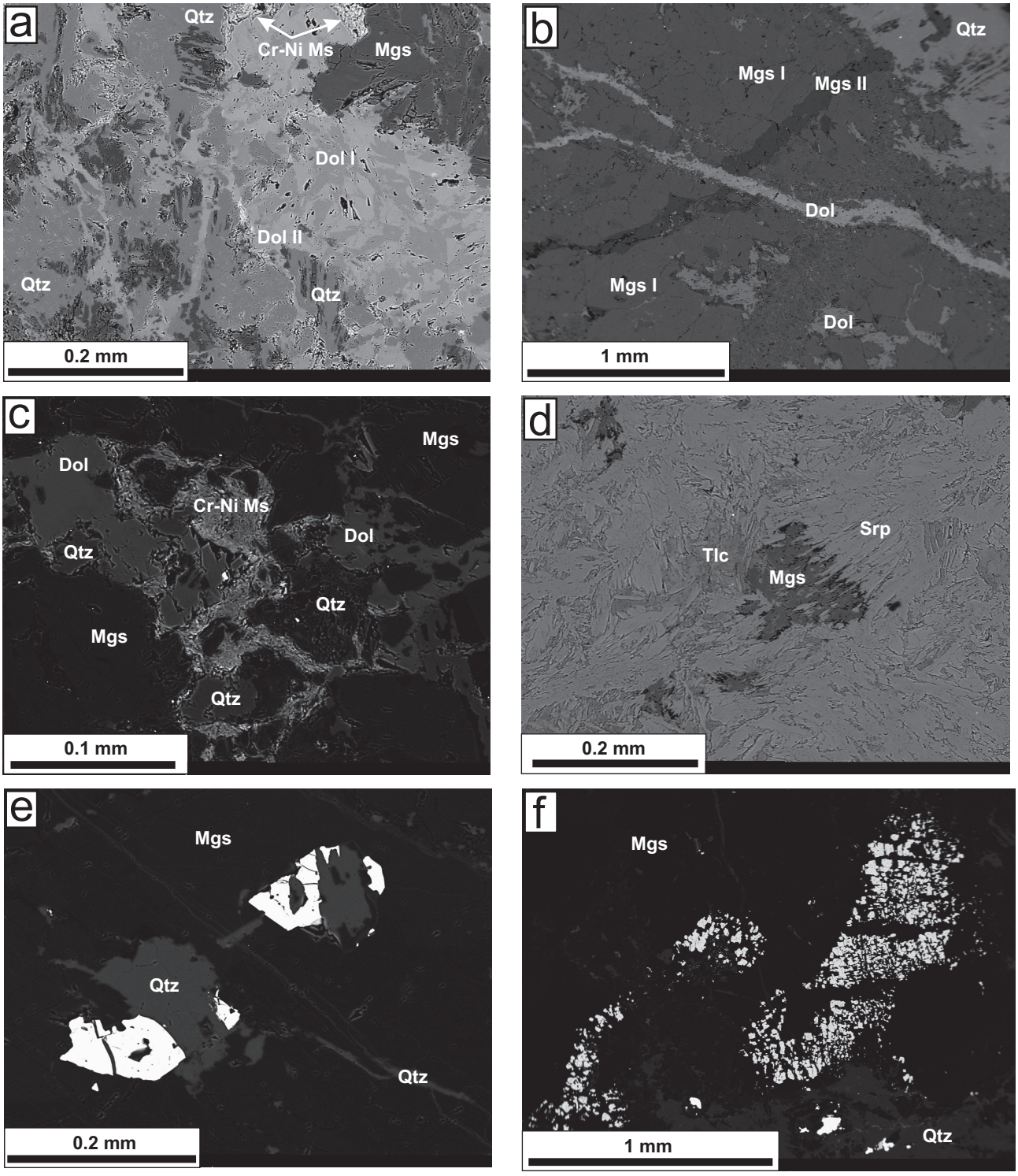

Fig. 2 Back-scattered electron images (BSE) of mineral associations in the Muránska Zdychava listvenite. **a –** Quartz (Qtz) and magnesite (Mgs) replaced by dolomite (Dol I, Dol II). The carbonates are replaced by Cr-Ni muscovite (Cr–Ni Ms) along the mineral rims. Quartz also overgrows relicts of magnesite I. **b –** Both of magnesite generations (Mgs) are cut by dolomite veinlets (Dol) and replaced by quartz aggregates (Qtz). **c –** Irregular aggregates of magnesite (Mgs), dolomite (Dol) and quartz are replaced by Cr–Ni-rich muscovite (Cr-Ni Ms). **d –** Magnesite (Mgs) relicts are overgrown and replaced by serpentine-group minerals (Srp), less frequently by talc (Tlc). Locally, talc forms intergrowths with serpentine--group minerals. **e –** Quartz (Qtz) fills tiny veinlets in magnesite (Mgs) and it replaces chromite grains (white). **f –** Chess-board breakdown of chromite (white) in magnesite (Mgs). Quartz (Qtz) forms irregular aggregates and veinlets in magnesite. Irregular white grains at bottom of the picture are sulphides.

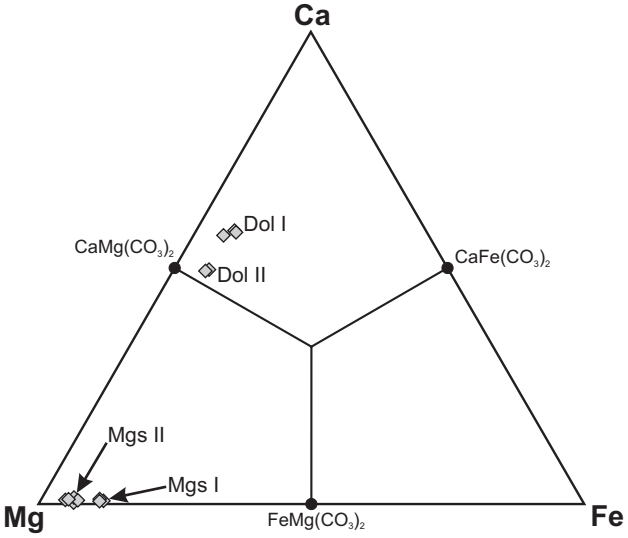

Fig. 3 Composition of magnesite and dolomite from Muránska Zdychava listvenite in ternary Mg–Ca–Fe diagram (at. %).

4.2.2. Cr–Ni-rich micas

The Cr–Ni-rich members of the mica group are characteristic minerals of the listvenite from Muránska Zdychava. They cause a green colour, especially of the L1 and L2 listvenite types. The micas form irregular, usually 20 to 100 μm large aggregates and veinlets of very fine platy crystals (up to 5 μm in size) in microcracks of magnesite, dolomite and quartz (Fig. 2c).

Tab. 2 Representative compositions of serpentine-group minerals (analyses 1 to 4) and talc (anal. 5) from the Muránska Zdychava listvenite

Mineral	Minerals of the serpentine group				Talc
Anal. #	1	2	3	4	5
SiO_2	44.34	43.83	43.32	42.69	61.94
Al_2O_3	0.60	0.89	0.75	1.34	0.00
Cr_2O_3	0.26	0.47	0.44	0.91	0.09
FeO	7.00	6.72	7.19	6.97	2.35
MgO	35.92	35.73	35.87	35.90	28.90
NiO	0.13	0.12	0.11	0.12	0.24
H_2O calc.	12.68	12.68	12.64	12.62	4.70
Total	100.94	100.44	100.32	100.55	98.23
empirical formulae					
Si	2.075	2.062	2.048	2.016	8.052
Al	0.033	0.050	0.042	0.075	
Cr	0.010	0.018	0.016	0.034	0.009
Fe	0.274	0.264	0.284	0.275	0.256
Mg	2.506	2.506	2.528	2.526	5.601
Ni	0.005	0.005	0.004	0.005	0.025
Sum *O*	2.828	2.842	2.874	2.915	5.891
OH	4.000	4.000	4.000	4.000	4.000
O	5.000	5.000	5.000	5.000	20.000
Sum of anions	9.000	9.000	9.000	9.000	24.000

The crystallochemical formulae are calculated on the basis of 5 oxygen (analyses 1–4) and 20 oxygen atoms (analysis 5). The H_2O content was estimaed in respect to stoichiometry of the ideal formulae

Chemical composition of the micas (Tab. 3) shows two compositional members: Cr–Ni-rich illite to muscovite and Cr–Ni-rich trioctahedral mica, both being characterized by unusually high contents of Cr^{3+} and Ni^{2+} in octahedral (*O*) site. The muscovite (Tab. 3, anal. 1 to 6) attains 7.6 to 11.0 wt. % Cr_2O_3 (0.44–0.64 *apfu* Cr) and 2.4 to 14.0 wt. % NiO (0.13–0.84 *apfu* Ni). Octahedral Al^{3+} is the dominant cation in the *O* site (0.87 to 1.19 *apfu*), whereas contents of octahedral Mg and Fe (assumed as Fe^{2+}) achieve only 0.15–0.23 and 0.03–0.15 *apfu*, respectively. Sum of trivalent octahedral cations ($^{O}M^{3+}$ = 1.34 to 1.71) is always higher than sum of the divalent ones ($^{O}M^{2+}$ = 0.44 to 1.07), whereas amount of interlayer cations (K, Na, Ca) attains only 0.57 to 0.73 *apfu* (0.55–0.69 *apfu* K), possibly due to the presence of H_3O^+ cation and/or interlayer vacancy. Therefore, the mica could be classified as dioctahedral, Cr–Ni-rich illite to muscovite.

Two analyses (Tab. 3, anal. 7 and 8) show the lowest Cr but the highest Ni contents: 5.7 to 6.5 wt. % Cr_2O_3 (0.36–0.40 *apfu* Cr) and 19.4 to 22.8 wt. % NiO (1.21–1.46 *apfu* Ni), respectively. On the contrary, these two compositions reveal the lowest contents of octahedral Al (0.55 to 0.69 *apfu*) and sum of interlayer cations (0.47 to 0.52 *apfu*; of this 0.46–0.50 *apfu* K). Nickel is a dominant divalent octahedral cation and $^{O}M^{2+} > {}^{O}M^{3+}$, whereby the sum of all octahedral cations is over 2.5 (2.54 to 2.67; Tab. 3, anal. 7 and 8). Consequently, they belong to Ni-dominant and (H_3O)-bearing or interlayer-deficient trioctahedral mica, close to the following formulae: $[K_{0.5}(H_3O)_{0.5}][Ni_{1.5}(Al,Cr)_1\square_{0.5}](AlSi_3)O_{10}(OH)_2$ or $[K_{0.5}\square_{0.5}][Ni_{1.5}(Al,Cr)_1\square_{0.5}](Al_{0.5}Si_{3.5})O_{10}(OH)_2$.

Compositional variations in both Cr–Ni-rich mica minerals indicate a dominant role for the muscovite–annite/phlogopite and muscovite–(alumino)celadonite (Tschermak-type) substitution mechanisms: $2{}^{O}M^{3+} + {}^{O}\square = 3{}^{O}M^{2+}$ and $^{O}M^{3+} + {}^{T}Al = {}^{O}M^{2+} + {}^{T}Si$, respectively (Fig. 4a). Chromium negatively correlates with nickel (Fig. 4b), consequently both $2{}^{O}Cr^{3+} + {}^{O}\square = 3{}^{O}Ni^{2+}$ and $^{O}Cr + {}^{T}Al = {}^{O}Ni + {}^{T}Si$ mechanisms possibly explain the incorporation of the Cr^{3+} and Ni^{2+} cations into the mica structure.

4.2.3. Chromite

Chromite is a widespread accessory mineral of the listvenite; it occurs as euhedral to subhedral, partly corroded crystals (usually 10 to 150 μm, exceptionally up to 1.2 mm in size) enclosed in magnesite I and II. Locally, chromite is cut by quartz veinlets (Fig. 2e). Moreover, some larger chromite crystals show "chess-board" breakdown patterns and partial replacement by magnesite (Fig. 2f). Chromite is dominated by Fe^{2+} (0.82 to 0.90 *apfu*) and

Cr (1.38 to 1.79 *apfu*) (Tab. 4, Fig. 5a–b); concentrations of Mg (0.05 to 0.12 *apfu*), Fe^{3+} (0.05 to 0.31 *apfu*) and Al (0.02 to 0.18 *apfu*) are relatively low. Magnesium reveals a strong negative correlation with Fe^{2+} (r = –0.98). Contents of Zn, Mn, Ti and V are subordinate (≤ 0.05 apfu).

Tab. 3 Representative compositions of Cr–Ni-rich micas from the Muránska Zdychava listvenite

Anal. #	1	2	3	4	5	6	7	8
SiO_2	46.05	46.55	48.35	46.71	45.74	44.07	42.56	40.94
TiO_2	0.00	0.00	0.05	0.04	0.00	0.00	0.00	0.03
Al_2O_3	22.87	21.94	20.36	18.82	18.61	18.22	15.05	13.72
Cr_2O_3	10.20	11.05	9.94	9.47	7.63	7.90	6.54	5.71
FeO	2.17	1.11	0.67	1.21	0.82	1.00	1.07	0.99
MnO	0.03	0.05	0.10	0.06	0.08	0.06	0.09	0.13
NiO	2.36	4.01	8.06	10.25	12.59	13.97	19.40	22.81
MgO	1.77	1.46	1.77	1.44	1.48	1.47	1.42	1.86
CaO	0.16	0.13	0.19	0.10	0.11	0.11	0.11	0.09
Na_2O	0.21	0.06	0.10	0.00	0.53	0.09	0.05	0.00
K_2O	7.60	7.78	6.81	6.46	6.27	5.76	5.02	4.57
H_2O calc.	4.26	4.27	4.33	4.19	4.12	4.03	3.86	3.76
Total	97.68	98.41	100.73	98.75	97.98	96.68	95.17	94.61
Formulae based on 10 O and 2(OH) anions								
Si	3.242	3.271	3.346	3.344	3.329	3.277	3.308	3.263
Al *T*	0.758	0.729	0.654	0.656	0.671	0.723	0.692	0.737
Sum *T*	4.000	4.000	4.000	4.000	4.000	4.000	4.000	4.000
Ti	0.000	0.000	0.003	0.002	0.000	0.000	0.000	0.002
Al *O*	1.140	1.088	1.006	0.932	0.925	0.874	0.686	0.552
Cr	0.568	0.614	0.544	0.536	0.439	0.465	0.402	0.360
Fe	0.128	0.065	0.039	0.072	0.050	0.062	0.070	0.066
Mn	0.002	0.003	0.006	0.004	0.005	0.004	0.006	0.009
Ni	0.134	0.227	0.449	0.590	0.737	0.836	1.213	1.462
Mg	0.186	0.153	0.183	0.154	0.161	0.163	0.165	0.221
Sum *O*	2.158	2.150	2.230	2.290	2.317	2.404	2.542	2.672
Ca	0.012	0.010	0.014	0.008	0.009	0.009	0.009	0.008
Na	0.029	0.008	0.013	0.000	0.075	0.013	0.008	0.000
K	0.683	0.698	0.601	0.590	0.582	0.546	0.498	0.465
Sum *I*	0.724	0.716	0.628	0.598	0.666	0.568	0.515	0.473
Al total	1.898	1.817	1.660	1.588	1.596	1.597	1.378	1.289
Sum M^{3+} *O*	1.708	1.702	1.550	1.468	1.364	1.339	1.088	0.912
Sum M^{2+} *O*	0.450	0.448	0.677	0.820	0.953	1.065	1.454	1.758

4.2.4. Sulphide minerals

The sulphide and sulphoarsenide phases are characteristic accessory minerals of the Muránska Zdychava listvenite (Fig. 6). The Ni–Co–Fe–(Cu–Pb) sulphide and sulphoarsenide minerals include pyrite, millerite, pyrrhotite, gersdorffite, cobaltite, polydymite, violarite, siegenite, pentlandite, chalcopyrite, and galena (Fig. 7a). Generally, they form scattered isometric grains (up to 0.2 mm) or veinlets (~1 to 0.1 mm) of discrete mineral (e.g., pyrite, millerite and pyrrhotite) or aggregates of several phases (e.g., millerite + pyrite + gersdorffite), usually in magnesite I. The

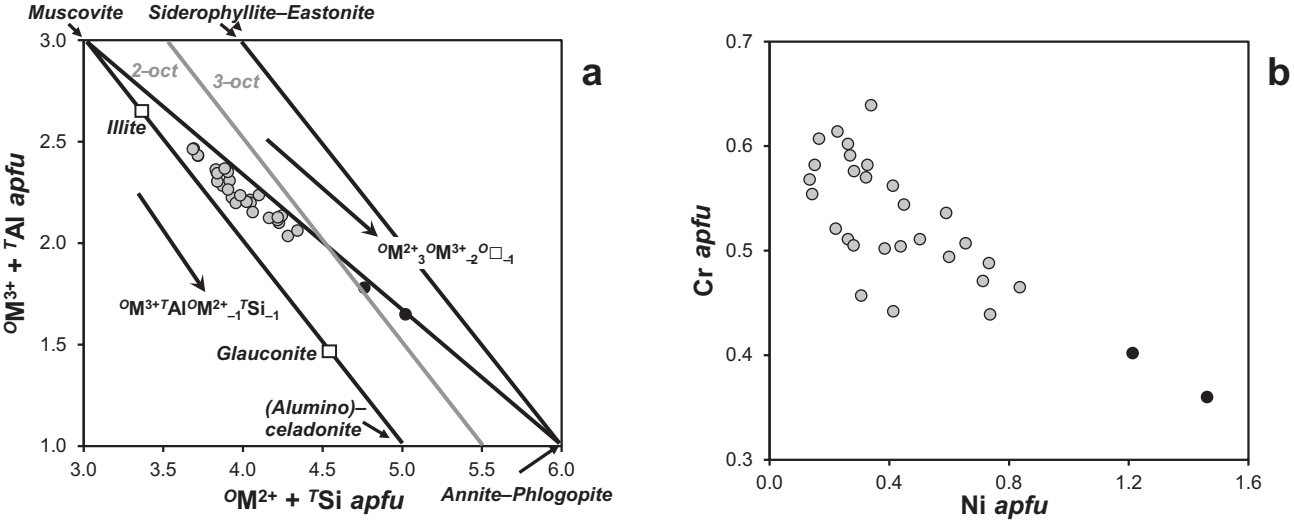

Fig. 4 Composition of Cr–Ni-rich illite to muscovite (grey circles) and Ni-dominant trioctahedral mica (black circles) from Muránska Zdychava listvenite (*apfu*). **a –** $^{O}M^{2+} + {}^{T}Si$ vs. $^{O}M^{3+} + {}^{T}Al$ diagram showing two principal substitution mechanisms of the micas: $2\,^{O}M^{3+} + {}^{O}\square = 3\,^{O}M^{2+}$ and $^{O}M^{3+} + {}^{T}Al = {}^{O}M^{2+} + {}^{T}Si$. Representative compositions of illite and glauconite (series names) are according to Rieder et al. (1998). The grey solid line indicates boundary between dioctahedral (2-oct) and trioctahedral (3-oct) micas. **b –** Ni vs. Cr substitution diagram (*apfu*).

Tab. 4 Representative compositions of chromite from the Muránska Zdychava listvenite

Anal. #	1	2	3	4	5	6	7	8
TiO_2	0.23	0.18	0.07	0.00	0.07	0.11	0.16	0.09
Al_2O_3	0.40	0.81	3.87	4.06	4.45	1.78	0.85	11.85
V_2O_3	0.11	0.29	0.15	0.20	0.25	0.19	0.20	0.00
Cr_2O_3	56.95	57.18	59.62	61.37	62.55	62.66	58.78	49.87
Fe_2O_3 *	11.16	10.71	5.31	3.23	1.87	4.76	9.45	4.61
FeO	29.30	29.44	29.01	28.71	28.99	29.24	29.37	27.81
ZnO	1.18	1.13	1.23	0.98	1.32	1.11	1.15	2.00
MnO	0.62	0.54	0.50	0.46	0.45	0.54	0.61	0.25
MgO	0.91	0.99	1.57	1.83	1.71	1.37	1.06	2.35
Total	100.84	101.27	101.34	100.84	101.66	101.76	101.63	98.85
atomic proportions (on basis of 4 O atoms)								
Ti	0.006	0.005	0.002	0.000	0.002	0.003	0.004	0.002
Al	0.017	0.035	0.163	0.171	0.186	0.076	0.036	0.491
V	0.003	0.008	0.004	0.006	0.007	0.006	0.006	0.000
Cr	1.660	1.655	1.688	1.739	1.756	1.786	1.693	1.385
Fe^{3+} *	0.310	0.295	0.143	0.087	0.050	0.129	0.259	0.122
Sum *B*	1.996	1.998	2.001	2.003	2.001	1.999	1.999	2.001
Fe^{2+}	0.903	0.901	0.868	0.860	0.860	0.881	0.894	0.817
Zn	0.032	0.031	0.033	0.026	0.035	0.029	0.031	0.052
Mg	0.050	0.054	0.084	0.098	0.090	0.074	0.058	0.123
Mn	0.019	0.017	0.015	0.014	0.014	0.017	0.019	0.007
Sum *A*	1.004	1.003	0.999	0.997	0.998	1.001	1.001	1.000
O	4.000	4.000	4.000	4.000	4.000	4.000	4.000	4.000

* calculated from stoichiometry

sulphide minerals occur mainly in the L1 and L2 types; they are less frequent in the L3 listvenite type.

Pyrite is the most widespread sulphide mineral of the listvenite; it forms usually anhedral, rarely subhedral crystals. The mineral shows elevated contents of nickel and cobalt: 0.7 to 5.1 wt. % Ni (≤ 0.10 *apfu*) and 0.6 to 2.2 wt. % Co (≤ 0.05 *apfu*). Nickel concentrations reveal slight negative correlation with Fe content (r = –0.67) but cobalt does not show any distinctive correlation with Fe or Ni (r < –0.50). Two pyrite generations have been recognized: older pyrite I, generally with lower Ni or Ni + Co (1.8 to 3.1 wt. %) and younger pyrite II that overgrows pyrite I (Fig. 6a), with higher Ni + Co (4.2 to 5.8 wt. %; Tab. 5).

Millerite is a relatively common mineral of the listvenite, forms discrete anhedral grains or veinlets in pyrite I. Locally, millerite occurs as trellis lamellae in a polydymite–violarite series mineral, as a breakdown product of primary Ni–Co–Fe–S solid-solution phase (Fig. 6b) or it is replaced by siegenite or gersdorffite (Fig. 6c). Millerite contains 0.6–4.2 wt. % Fe (≤ 0.07 *apfu*), low concentrations of Co (max. 0.7 wt. %) and negligible admixtures of Pb and Cu (Tab. 5). The millerite trellis lamellae in polydymite–violarite show elevated contents of Fe + Co (3.4–4.9 wt. %) in comparison to discrete grains of millerite (Tab. 5). The most distinct $FeNi_{-1}$ substitution in millerite displays very high negative correlation (–0.98); relatively strong

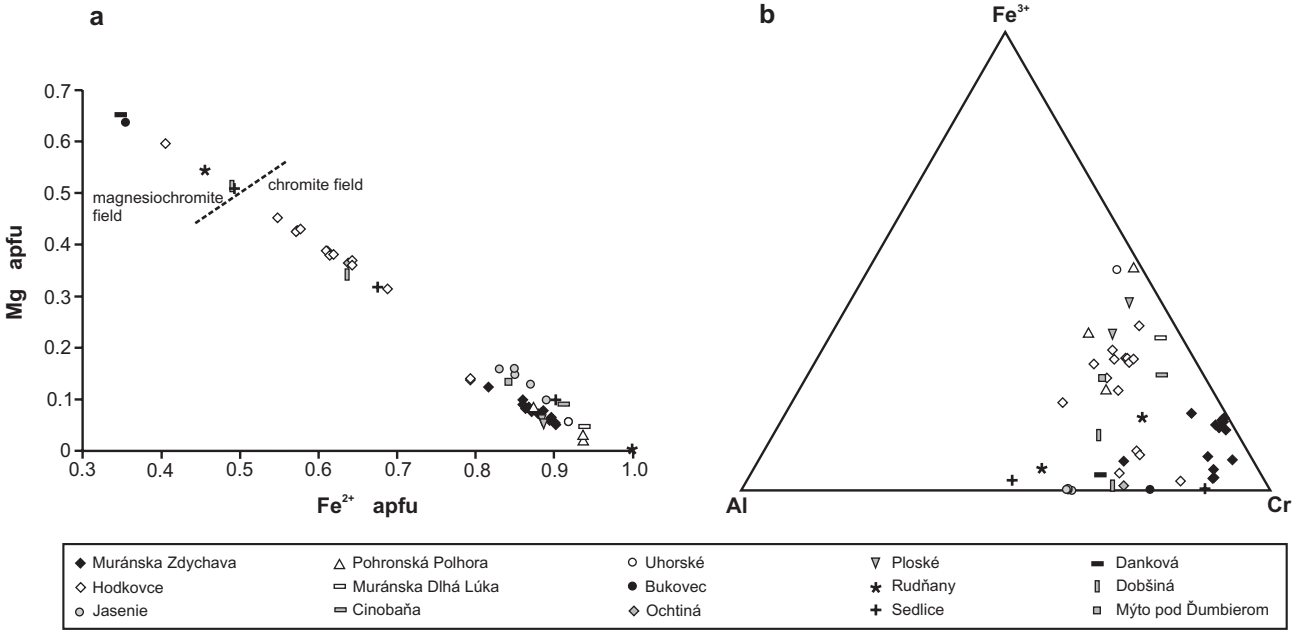

Fig. 5 Chromite compositions (*apfu*) from the Muránska Zdychava listvenite compared with Cr-rich spinels from other ultrabasic bodies in the Western Carpathians (Rojkovič 1985; Spišiak at al. 1994; Mikuš and Spišiak 2007). **a** – Fe^{2+} vs. Mg diagram. **b** – Al–Fe^{3+}– Cr diagram.

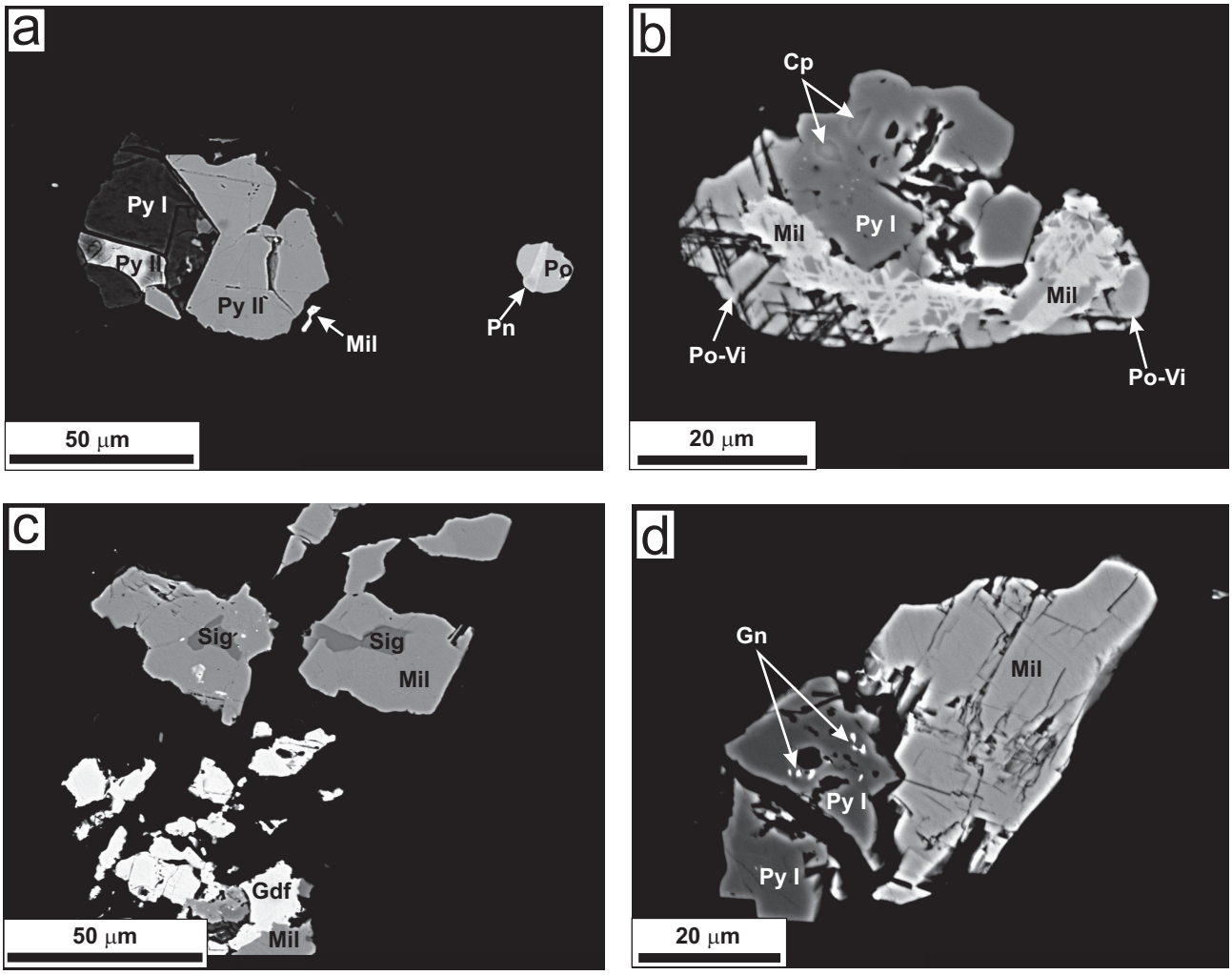

Fig. 6 Back-scattered electron images (BSE) of sulphide minerals in the Muránska Zdychava listvenite. **a –** Fractured pyrite I (Py I) overgrown by pyrite II (Py II). Millerite (Mil) forms small irregular grain at rim of pyrite aggregate, pentlandite lamella (Pn) occurs in isometric pyrrhotite grain (Po). **b –** Pyrite I (Py I) with chalcopyrite inclusions (Cp) is overgrown by millerite aggregate (Mil) and minerals of polydymite–violarite series (Po-Vi). Trellis-type lamellae of millerite in polydymite–violarite indicate exsolution breakdown of a primary solid solution. **c –** Millerite (Mil) is cut by siegenite veinlets (Sig), whereas gersdorffite (Gdf) replaces the both minerals. **d –** Pyrite I (Py I) containing galena inclusions (Gn) is associated with millerite (Mil).

correlations Co vs. Ni and Co vs. Fe (–0.79 and –0.78, respectively) indicate $CoNi_{-1}$ and $CoFe_{-1}$ substitution mechanisms.

Thiospinel minerals of the *polydymite–violarite* series and *siegenite* were identified in the listvenite. The polydymite–violarite members overgrow pyrite I or they form discrete grains. The millerite lamellae in polydymite–violarite matrix (Fig. 6b) indicate the exsolution breakdown of primary Ni–Co–Fe–S solid-solution phase. The mineral of the polydymite–violarite series reveals increased contents of Co (1.9 to 3.4 wt. %, 0.10 to 0.17 apfu; Tab. 5, Fig. 7b). Excellent negative correlations between Ni and Fe or Co (up to –1.0) document the $FeNi_{-1}$ and $CoNi_{-1}$ substitution mechanisms.

Siegenite is the most common thiospinel mineral in the listvenite. It forms overgrowths or fracture fillings of discrete millerite grains (Fig. 6c). Siegenite shows high iron content (7.3 to 10.0 wt. %, 0.40 to 0.55 *apfu* Fe; Tab. 5) and Fe partly substitutes Ni (r = –0.84). Therefore, studied siegenite represents intermediate phase between siegenite end-member ($CoNi_2S_4$), violarite ($FeNi_2S_4$) and an unnamed $CoNiFeS_4$ phase (Fig. 7b).

Gersdorffite occurs in local accumulations of discrete grains in association with millerite and thiospinels; in some cases it replaces millerite aggregates (Fig. 6c). Gersdorffite reveals wide variations in Co (0.0 to 11.7 wt. %, ≤ 0.33 *apfu*) and Fe (0.5 to 2.2 wt. %, 0.02 to 0.05 *apfu*); the content of Sb is negligible, max. 0.3 wt. % (Tab. 5).

Cobaltite is a relatively rare mineral of the listvenite, it forms discrete anhedral crystals (~15 μm across) in magnesite I. It shows relatively high content of Ni (~9 wt. %,

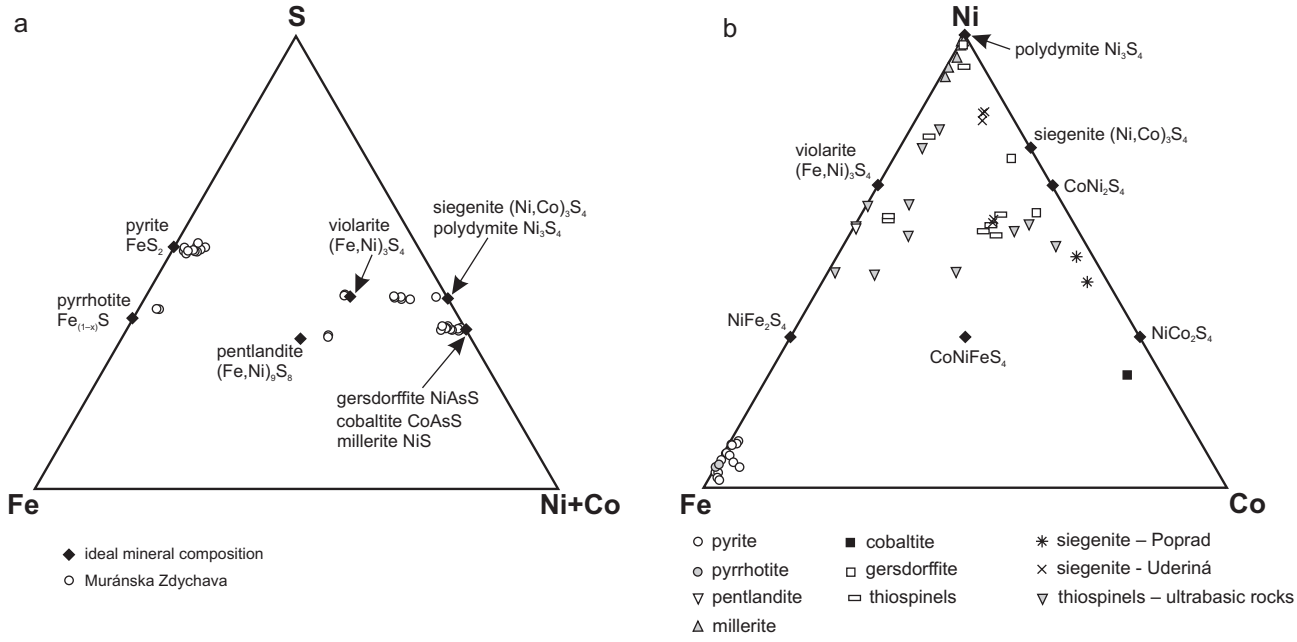

Fig. 7 Compositions of sulphide minerals (*apfu*) from Muránska Zdychava listvenite compared with those from the Alpine hydrothermal veins (Uderiná, Poprad) and other ultrabasic bodies in the Western Carpathians (Rojkovič 1985; Ferenc and Rojkovič 2001; Ferenc et al. 2014). **a –** Fe–S–Ni + Co diagram. **b –** Fe–Ni–Co diagram.

0.25 *apfu*) and Fe (~3 wt. %, 0.08 *apfu*) (Tab. 5). Other uncommon sulphide minerals are *pyrrhotite, pentlandite, chalcopyrite*, and *galena*. Pyrrhotite forms tiny grains scattered in magnesite I or intergrowths with pentlandite laths (Fig. 6a). Pyrrhotite contains 3.3 to 3.8 wt. % Ni (~0.05 apfu; Tab. 5). Chalcopyrite and galena were identified as minute inclusions (2–5 μm) in pyrite I (Fig. 6b, d).

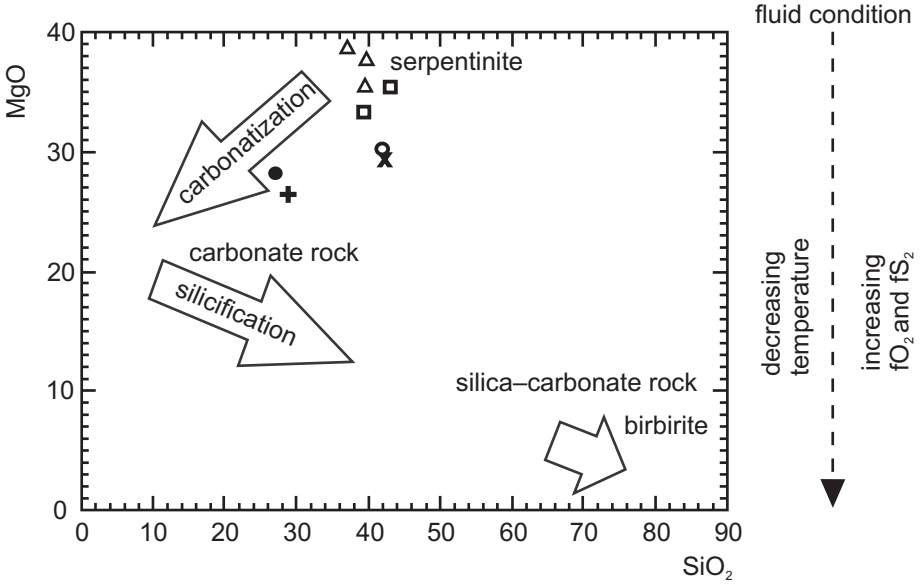

● 1 Muránska Zdychava listvenite (L1)

✚ 2 Muránska Zdychava listvenite (L2)

✘ 3 Muránska Zdychava listvenite (L3)

○ 4 Talc–carbonate rock, Muránska Dlhá Lúka (FMDL-35, Ivan 1985)

□ 5 Antigorite–talc serpentinite, Muránska Dlhá Lúka (MDL-1, 2, Hovorka 1965)

△ 6 Various serpentinites (Styles et al. 2014)

Fig. 8 SiO_2 vs. MgO binary diagram (wt. %) showing chemical changes during alteration of serpentinites (according Akbulut et al. 2006). Explanations 1–5 represent analyses in Tab. 6.

4.3 Geochemical characterization of the listvenite

Chemical composition of the L1 to L3 listvenite types (Tab. 6) shows high contents of MgO (26 to 30 wt. %), Fe_2O_3 (6 to 7 wt. %), C in carbonate form (5 to 10 wt. %), Cr_2O_3 (~0.3 wt. %), NiO (~0.2 wt. %), but very low contents of SiO_2 (27 to 41 wt. %), Al_2O_3 (~0.5 wt. %), Na_2O (< 0.01 wt. %) and K_2O (< 0.15 wt. %); Ca content varies between 0.1 and 3.2 wt. % CaO. The listvenite displays elevated concentrations of As and Co, but contents of Rb,

Sr, Ba and other trace elements (including REE) are very low (Tab. 6).

The listvenites at Muránska Zdychava provide a good example of a polystage transformation of the primary ultrabasic rock, as documented in the studied L1 to L3 rock types, which demonstrate various degrees of alteration (Tab. 6). The L3 type represents an incipient alteration stage with highest contents of SiO_2, MgO, and Cr_2O_3, typical of ultrabasic rocks (Fig. 8). The L1 and L2 types assume more advanced alteration with low SiO_2 but with distinctly higher LOI (around 35 wt. %), reflecting mainly CO_2 and H_2O in carbonates (magnesite and dolomite) and hydrated silicate minerals (Cr–Ni-rich micas, serpentine group minerals and talc). On the contrary, all three listvenite types show very low contents of REE and other rare metals (e.g., Ga, Zr or U); concentrations of these trace elements were not distinctly influenced by alteration of primary ultrabasic rock (Tab. 6).

5. Discussion

The geochemistry and the alteration trends of the listvenites from Muránska Zdychava are generally comparable to the hydrothermal–metasomatic transformation in some other occurrences of listvenitized ultrabasic rocks (e.g., Hovorka et al. 1985; Akbulut et al. 2006; Styles et al. 2014; Figs 8–9). Ultrabasic or basic magmatic protolith (gabbros, basalts...) is essential for origin of the listvenites (e.g., Sazonov 1978; Dinel et al. 2008; Buckman and Ashley 2010). Two principal types of ultramafic rocks occur in the Western Carpathians (Hovorka

Tab. 5 Representative compositions of sulphide minerals from the Muránska Zdychava listvenite

Anal. #	Fe	Co	Ni	Pb	Cu	Sb	As	S	wt. %	Mineral
1	44.81	0.76	1.05	0.28				52.82	99.72	pyrite I
2	44.84	0.14	2.98	0.13				52.28	100.37	pyrite I
3	44.21	1.19	0.74	0.00				52.97	99.11	pyrite I
4	43.30	0.81	3.46	0.10				52.56	100.24	pyrite II
5	41.58	0.65	4.72	0.13				52.53	99.62	pyrite II
6	41.18	2.24	2.24	0.00				53.49	99.16	pyrite II
7	40.79	0.73	5.07	0.00				53.32	99.91	pyrite II
8	42.17	1.44	2.71	0.00				53.17	99.50	pyrite II
9	4.20	0.67	58.99	0.19	0.00			36.24	100.30	millerite
10	3.45	0.36	59.92	0.15	0.07			35.84	99.79	millerite
11	2.68	0.71	62.36	0.00	0.16			35.85	101.76	millerite
12	0.62	0.18	63.43	0.14	0.00			35.19	99.56	millerite
13	1.39	0.00	62.85	0.00	0.07			35.01	99.31	millerite
14	19.13	3.36	33.57	0.21	0.06		0.24	42.10	98.67	violarite
15	10.18	2.62	44.96	0.00	0.06		0.11	42.24	100.17	violarite
16	2.15	1.93	52.85	0.00				41.96	98.89	polydymite
17	9.95	14.45	32.19	0.22				41.87	98.68	siegenite
18	8.91	16.12	31.71	0.19				41.64	98.58	siegenite
19	7.32	15.57	35.00	0.21				41.84	99.94	siegenite
20	1.69	8.00	25.67	0.07		0.32	44.86	19.40	100.01	gersdorffite
21	2.23	11.70	21.34	0.11		0.29	44.22	19.40	99.30	gersdorffite
22	0.55	0.03	35.76	0.00		0.06	43.60	19.98	99.97	gersdorffite
23	2.87	24.68	8.94	0.00			44.87	19.72	101.08	cobaltite
24	55.00	0.02	3.30	0.22			0.09	38.53	97.16	pyrrhotite
25	55.75	0.13	3.80	0.10			0.00	39.43	99.21	pyrrhotite
26	26.27	0.13	38.02	0.22	0.00			33.05	97.69	pentlandite
27	26.35	0.26	37.82	0.10	0.08			32.57	97.19	pentlandite
atomic proportions										
1	0.970	0.016	0.022	0.002				1.991	3.000	pyrite I
2	0.968	0.003	0.061	0.001				1.967	3.000	pyrite I
3	0.959	0.024	0.015	0.000				2.001	3.000	pyrite I
4	0.935	0.017	0.071	0.001				1.977	3.000	pyrite II
5	0.902	0.013	0.098	0.001				1.986	3.000	pyrite II
6	0.891	0.046	0.046	0.000				2.017	3.000	pyrite II
7	0.879	0.015	0.104	0.000				2.002	3.000	pyrite II
8	0.912	0.030	0.056	0.000				2.003	3.000	pyrite II
9	0.068	0.010	0.904	0.001	0.000			1.017	2.000	millerite
10	0.056	0.006	0.925	0.001	0.001			1.012	2.000	millerite
11	0.043	0.011	0.947	0.000	0.002			0.997	2.000	millerite
12	0.010	0.003	0.986	0.001	0.000			1.001	2.000	millerite
13	0.023	0.000	0.978	0.000	0.001			0.998	2.000	millerite
14	1.047	0.174	1.749	0.003	0.003		0.010	4.014	7.000	violarite
15	0.552	0.135	2.319	0.000	0.003		0.004	3.988	7.000	violarite
16	0.118	0.101	2.764	0.000				4.017	7.000	polydymite
17	0.547	0.753	1.685	0.003				4.012	7.000	siegenite
18	0.491	0.842	1.664	0.003				4.000	7.000	siegenite
19	0.399	0.805	1.817	0.003				3.976	7.000	siegenite
20	0.050	0.225	0.725	0.001		0.004	0.992	1.003	3.000	gersdorffite
21	0.066	0.331	0.606	0.001		0.004	0.984	1.008	3.000	gersdorffite
22	0.016	0.001	1.002	0.000			0.957	1.025	3.000	gersdorffite
23	0.084	0.684	0.249	0.000			0.978	1.005	3.000	cobaltite
24	0.820	0.001	0.047	0.001			0.001	1.000	1.869	pyrrhotite
25	0.812	0.005	0.053	0.000			0.000	1.000	1.870	pyrrhotite
26	3.715	0.018	5.117	0.008	0.000			8.142	17.000	pentlandite
27	3.752	0.035	5.123	0.004	0.010			8.076	17.000	pentlandite

The crystallochemical formulae are calculated on the basis of 2 atoms (analyses 9–13), 3 atoms (1–8; 20–23), 7 atoms (15–19), 17 atoms (26–27), and 1 S atom (24–25)

Tab. 6 Whole-rock chemical analyses of the Muránska Zdychava listvenite (L1 to L3 types)

	L-1	L-2	L-3	FMDL-35	MDL-1	MDL-2
SiO_2	26.73	28.01	41.46	42.40	38.93	42.45
TiO_2	<0.01	<0.01	<0.01	0.02	<0.01	<0.01
Al_2O_3	0.52	0.51	0.55	1.41	3.31	3.88
Fe_2O_{3tot}	6.76	6.44	6.13	8.05	7.90	6.60
MgO	28.71	26.01	29.97	30.08	32.99	34.93
CaO	0.44	3.22	0.07	0.43	2.72	0.54
MnO	0.10	0.13	0.07	0.12	0.12	0.06
Na_2O	<0.01	<0.01	<0.01	0.07	0.18	0.93
K_2O	0.14	0.14	<0.01	0.07	0.10	0.33
P_2O_5	<0.01	0.04	<0.01	0.01	0.01	<0.01
Cr_2O_3	0.276	0.263	0.361	n.a.	n.a.	n.a.
LOI	35.60	34.60	20.60	17.72	13.62	11.02
Total	99.28	99.36	99.21	100.38	99.88	100.74
TOT/C	10.00	9.80	4.61	n.a.	n.a.	n.a.
TOT/S	0.03	<0.02	0.03	0.12	n.a.	n.a.
Cr				1740	3050	3340
Ni	1546	1408	1798	1235	1875	1503
Co	89.1	76.4	87.8	54	110	124
Cu	18.9	112.5	20.9	18	n.a.	n.a.
Pb	3.8	24.2	1.6	n.a.	n.a.	n.a.
Zn	49	62	35	101	n.a.	n.a.
Sb	5.6	3.9	0.8	n.a.	n.a.	n.a.
Bi	2.1	1.4	2.8	n.a.	n.a.	n.a.
As	384.9	59.4	237.8	n.a.	n.a.	n.a.
Rb	14.4	14.6	0.2	n.a.	n.a.	n.a.
Cs	3.8	1.9	0.2	n.a.	n.a.	n.a.
Sr	16	91.8	1.9	n.a.	n.a.	n.a.
Ba	14	16	5	n.a.	n.a.	n.a.
Ga	1.1	0.9	1.2	n.a.	n.a.	n.a.
V	24	20	25	25	58	52
U	0.1	<0.1	0.2	n.a.	n.a.	n.a.
Sc	6	5	6	n.a.	14	2
Zr	1.4	0.1	0.2	n.a.	n.a.	n.a.
Y	0.4	0.4	0.2	n.a.	n.a.	n.a.
La	0.3	<0.1	0.2	n.a.	n.a.	n.a.
Ce	0.3	<0.1	0.2	n.a.	n.a.	n.a.
Dy	<0.05	<0.05	0.06	n.a.	n.a.	n.a.
Yb	0.06	<0.05	<0.05	n.a.	n.a.	n.a.
Au	2.8	8.7	2.1	n.a.	n.a.	n.a.

Fe_2O_3tot – total Fe as Fe_2O_3, n.a. – not analyzed.
oxides, C and S in wt. %., trace elements in ppm and Au in ppb
L 1–3 original analyses; FMDL-35– talc–carbonate rock, Muránska Dlhá Lúka (Ivan 1985); MDL-1– antigorite serpentinite, MDL-2– talc–antigorite serpentinite (Hovorka 1965)

1978): (1) basic to ultrabasic rocks of the gabbro–peridotite formation with characteristic Fe, Mn and Ti enrichment and (2) ultrabasic rocks of the peridotite formation with elevated Mg, Cr and Ni contents, and lower Si and alkalis compared with (1). Absence of ilmenite and presence of chromite as well as Ni–Co sulphide minerals (*sensu* Hovorka 1978; Rojkovič 1985) enable to assign the protolith of the Muránska Zdychava listvenite to the ultrabasic rocks of the peridotite formation.

The second principal prerequisite for the listvenite origin represent brittle tectonics and propagation of faults in the host rock, serving as channels for effective circulation of the mineralizing fluids (Hansen et al. 2005).

Moreover, listvenites are commonly associated with vein or metasomatic ore mineralizations, as for example in Ural Mts. (Sazonov 1975) or in the Rocky Mts. (Hansen et al. 2005). In the Western Carpathians, Cr-rich muscovite (fuchsite) and quartz-rich listvenites were described mainly from siderite–quartz–sulphide hydrothermal deposits (Dobšiná, Rudňany, Slovinky, Gelnica, Mlynky and other occurrences) of the Gemeric Superunit; rarely they occur in ultrabasic rocks at the Muránska Dlhá Lúka, Veporic Superunit and Jasenie in the Tatric Superunit (Ivan 1984, 1985; Grecula et al. 1995 and references therein).

Based on geochemical and mineralogical characteristics, the studied listvenite body near Muránska Zdychava originated during three principal evolution stages: (1) peridotite stage, (2) serpentinization stage, and (3) hydrothermal–metasomatic stage (listvenitization).

Rock-forming magmatic minerals of the primary ultrabasic rock, most probably peridotite (stage 1) were almost completely transformed to younger assemblages (2) and (3). However, relicts of Mg-bearing chromite, rare pyrrhotite with pentlandite lamellae and pyrite I with chalcopyrite exsolutions are still preserved.

The serpentinization stage (2) is represented by serpentine minerals (with later magnesite I + quartz assemblage) is partly preserved mainly in the L3 type of the listvenite (Tab. 6, Fig. 8). Moreover, we suggest a partial dissolution of the older sulphide minerals, mobilization of Ni, Co, Fe, S, As and their new precipitation in the form of pyrite II + millerite + siegenite + polydymite + violarite + gersdorffite + cobaltite mineral assemblage during serpentinization. The secondary origin of sulphide and sulphoarsenide minerals due to serpentinization is generally a characteristic feature of ultramafic bodies in the Western Carpathians (Rojkovič 1985). Precipitation of Ni and Co sulphoarsenides is typical of advanced serpentinization to listvenitization, and this process can be an effective for Ni and Co mobilization and accumulation, perhaps up to economic concentrations, such as in the Dobšiná deposit, Slovakia

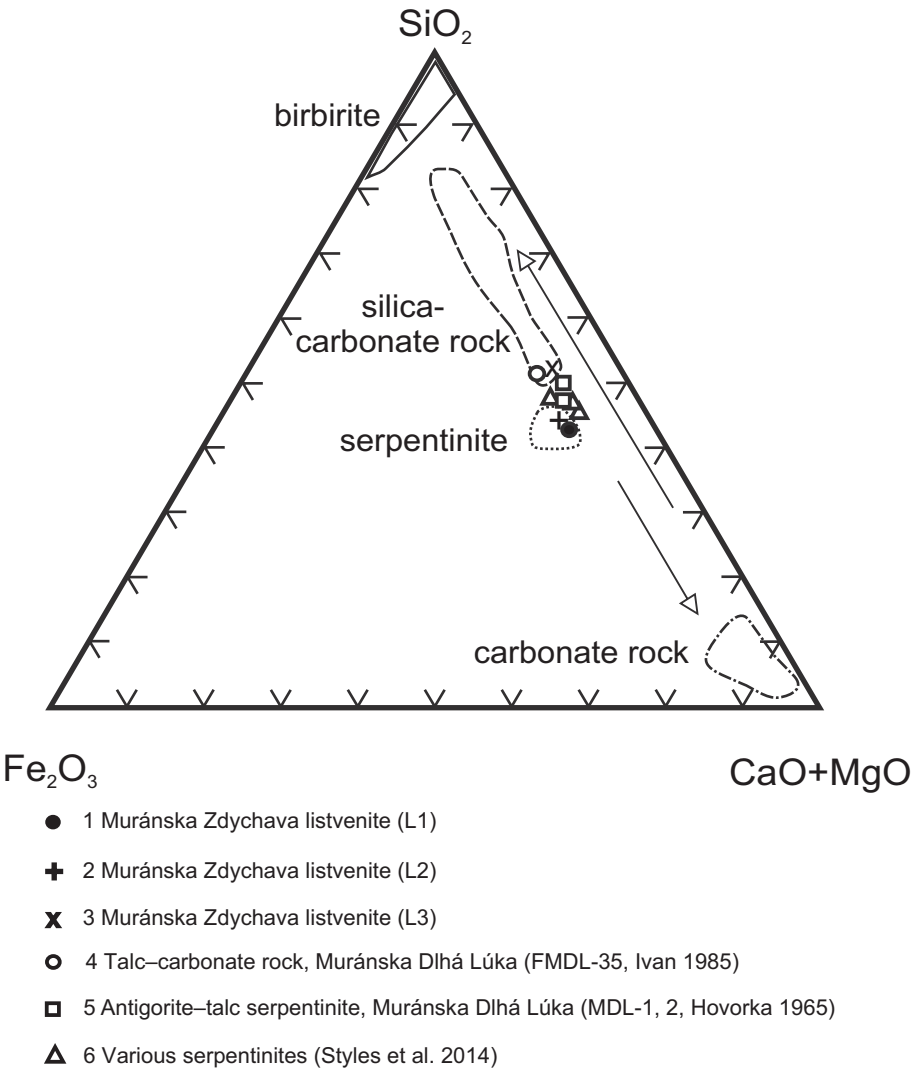

Fig. 9 Ternary diagram Fe_2O_3 – SiO_2 – MgO + CaO with alteration trends of serpentinites and fields of altered rocks according to Akbulut et al. (2006). Explanations 1–5 represent analyses in Tab. 6.

(Ivan and Hovorka 1980), Kamaishi mining district, Japan (Shiga 1987) or Bou Azzer deposit, Morocco (Alansari et al. 2015). Millerite and polydymite were observed also in steatitized abyssal peridotites of the Mid-Atlantic Ridge, where increased Si and decreased H_2 activities enable precipitation of high sulphur-fugacity sulphides (Klein and Bach 2009).

The third, advanced hydrothermal–metasomatic stage (listvenitization) represent mainly the L1 and L2 types of the listvenite with dominant magnesite I–II + dolomite I–II + quartz + Cr–Ni-rich micas. This alteration of serpentinized rocks by CO_2-rich fluids is illustrated by the following reaction: $Mg_3Si_2O_5(OH)_4 + 3\ CO_2 = 3\ MgCO_3 + 2\ SiO_2 + 2\ H_2O$ (Halls and Zhao 1995). Generally, alteration of ultrabasic rocks to listvenites involves two basic processes (Akbulut et al. 2006; Figs 8–9). (1) Silicification is caused by fluids rich in SiO_2 and H_2O at relatively low pH. This process leads to quartz ± carbonate rocks with unusually high SiO_2 contents, up to 80 wt. % (birbirites). (2) Carbonatization represents the alteration by fluids enriched in CO_2, H_2O and Ca^{2+}, with higher pH, as well as decreased fS_2 and fO_2 in comparison with the silicification. The altered ultrabasic rocks reveal low SiO_2 but high CaO and MgO contents. In our case, the final hydrothermal–metasomatic transformation of the Muránska Zdychava listvenite included relatively rapid decrease in SiO_2, slight decrease in MgO and only insignificant increase in K_2O. Strong enrichment of total carbon in L1–L2 analyses (Tab. 6) is unambiguously a manifestation of high CO_2 content in fluids responsible for the listvenitization.

The Cr–Ni-rich micas precipitated during the listvenitization of the investigated ultrabasic rock, in association with magnesite, dolomite and quartz (Fig. 2a, c). The micas from the Muránska Zdychava listvenite contain the highest values of Ni ever reported in the mica-group minerals (up to 22.8 wt. % NiO or 1.46 *apfu* Ni); the Cr concentrations are also relatively high (up to 11.0 wt. % Cr_2O_3 or 0.64 *apfu*). The micas were formed under a significant Al and K deficit (Tab. 6),

which caused their small volume in listvenite and unusual composition.

Similar micas with unusually high Cr and Ni contents were formed under analogous conditions in transformed ultrabasic rocks. The maximum Ni content in previously reported chromian muscovite attained 8.75 wt. % NiO (0.53 *apfu*), together with up to 13.5 wt. % Cr_2O_3 (0.75 *apfu*); it occurs in quartz veins and stockworks that traverse the ophiolitic emerald-hosting, carbonate-altered ultramafic rocks in the Swat Valley, the Indus suture, NW Pakistan (Arif and Moon 2007). Nickel-rich phlogopite (up to 4.3 wt. % NiO or 0.26 *apfu*) occurs in association with Ni-bearing sodium amphibole, chlorite and talc in Ni-rich lateritic rocks transformed from serpentinites in Studena Voda Fe–Ni ore deposit of the Vardar ophiolite zone in Macedonia (Maksimović and Pantó 1982). Muscovite with 5.5 wt. % Cr_2O_3 and 2.0 wt. % NiO (0.29 *apfu* Cr and 0.11 *apfu* Ni) was described from quartz–magnesite listvenites with chromite in the Setogawa Group, east of Nagoya, Japan (Takasawa et al. 1976). Despite the lack of textural evidence, we assume partly dissolved chromite as a main source of Cr. Similarly, primary Ni-bearing silicate minerals (especially serpentinized olivine?) or older Ni-rich sulphide minerals (probably pentlandite) could have served as a principal source of Ni in the micas. Analogous partial dissolution and replacement of primary chromite by Cr–Ni-rich muscovite was documented in listvenitized ultrabasic rock from Swat Valley, Pakistan (Arif and Moon 2007).

The listvenitization of ultrabasic rocks represents a hydrothermal–metasomatic process under the greenschist-facies metamorphic conditions, at ~290 to 340 °C and ~100 to 300 MPa (eg., Halls and Zhao 1995; Plissart et al. 2009; Bagherzadeh et al. 2013). In the studied listvenite body near Muránska Zdychava, this process was probably connected with Alpine (Late Cretaceous), late-orogenic uplift of the Veporic Superunit crystalline basement and retrograde metamorphism at temperature of 350 to 500 °C and pressure of 200 to 400 MPa (Kováčik et al. 1996). Consequently, we assume that the final listvenite stage took place at ~200 MPa and less than 350 °C. These conditions corresponded to en-block exhumation of Veporic Superunit between 80 and 55 Ma, resulting from the underthrusting of the Tatric–Fatric continental crust from the north. In this time period, central part of the Veporic Superunit cooled down from 350 °C to 60 °C (Vojtko et al. 2016). The NE–SW and NW–SE trending fault structures played a key role during the listvenitization; they presumably channelled the CO_2-rich fluids that transformed the serpentinized peridotite into magnesite I + dolomite I + quartz + Cr–Ni-rich muscovite. Contemporaneously with the listvenite origin, some hydrothermal siderite and quartz–sulphide mineralizations grew on the fault zones of metamorphic rocks in the Muránska Zdychava area (Maťo et al. 2005). The Late Cretaceous age (~70 to 80 Ma) and presence of CO_2-rich fluids was documented for analogous hydrothermal mineralization in adjacent Gemeric Superunit of the Western Carpathians (Hurai et al. 2008). The youngest mineralization of the studied listvenite (younger hydrothermal, *sensu* Hovorka et al. 1985) is represented by veinlets of white calcite without sulphide minerals.

6. Conclusions

1) The listvenite near Muránska Zdychava originated from primary magmatic ultrabasic body (probably peridotite) during three principal evolution stages: (1) magmatic stage, (2) serpentinization stage, and (3) hydrothermal–metasomatic stage (listvenitization).
2) The final listvenitization stage (3) took place during Alpine (Late Cretaceous) late-orogenic uplift and retrograde metamorphism of the Veporic Superunit crystalline basement; its assumed P–T conditions were ~200 MPa and ≤ 350 °C.
3) The NE–SW and NW–SE trending fault structures likely played a key role during the listvenitization, as they provided channels for circulation of CO_2-rich fluids that transformed the serpentinized peridotite into carbonate–quartz-rich listvenite.
4) The micas from the Muránska Zdychava listvenite represent Cr–Ni-rich illite to muscovite and Ni-dominant trioctahedral mica (probably a new, formally unapproved mineral species). They contain the highest values of Ni ever reported in the mica-group minerals (up to 22.8 wt. % NiO; or 1.46 *apfu* Ni), the Cr concentrations attain 11.0 wt. % Cr_2O_3 (0.64 *apfu*). Chromium shows negative correlation with Ni; two principal substitution mechanisms occur in the micas: $2\,{}^{O}M^{3+} + {}^{O}\square = 3\,{}^{O}M^{2+}$ and ${}^{O}M^{3+} + {}^{T}Al = {}^{O}M^{2+} + {}^{T}Si$.
5) Chromite and Ni–Co–Fe sulphide minerals (mainly pentlandite, millerite, polydymite, violarite, siegenite and gersdorffite) were the main sources for the formation of Cr–Ni-rich micas during the final hydrothermal–metasomatic stage of the listvenite formation, together with their intense carbonatization.

Acknowledgements. This work was supported by the Slovak Research and Development Agency projects APVV-0081-10 and APVV-15-0050, as well as the Ministry of Education, Slovak Republic (VEGA-1/0255/11 and VEGA-1/0650/15). Authors thank V. Kollárová for her assistance during the electron-microprobe work and both reviewers, L. Ackerman and P. Ivan, for their valuable comments that improved the manuscript.

References

Akbulut M, Pişkin Ö, Karayiğit AI (2006) The genesis of the carbonatized and silicified ultramafics known as listvenites: a case study from the Mihaliççik region (Eskişehir), NW Turkey. Geol J 41: 557–580

Alansari A, Bhilisse M, Maacha L, Soulaimani A, Michard A, Ennaciri A (2015) The Co, Ni, Cr and S mineralisation during serpentinization process in the Bou Azzer ore deposits (Anti-Atlas, Morocco). J Tethys 3: 216–236

Arif M, Moon CJ (2007) Nickel-rich chromian muscovite from the Indus suture ophiolite, NW Pakistan: implications for emerald genesis and exploration. Geochem J 41: 475–482

Bagherzadeh RM, Mirnejad H, Eshback P, Karimpour MH (2013) Investigation of Au-bearing listvenite using mineralogy, geochemistry, fluid inclusion and stable isotopes (oxygens, carbon and sulphur) in ophiolite-melange zone of East Iran, Hangaran area, South Birjand. Scient Quart J Geosci 22: 131–144

Bezák V (1982) Metamorphic and granitic complexes in the Kohút Belt of Veporic Unit. Geol Práce, Správy 78: 65–70 (in Slovak)

Bezák V, Hraško Ľ, Konečný V, Kováčik M, Madarás J, Plašienka D, Pristaš J (1999) Geological map of the Slovenské Rudohorie Mts. – western part, 1 : 50 000. State Geological Institute of D. Štúr, Bratislava (in Slovak)

Buckman S, Ashley PM (2010) Silica–carbonate (listwanites) related gold mineralisation associated with epithermal alteration of serpentinite bodies. In: Buckman S, Blevin PL (eds) New England Orogen 2010. University of New England, Armidale, NSW, Australia, pp 94–105

Dinel E, Fowler AD, Ayer J, Still A, Tylee K, Barr E (2008) Lithogeochemical and stratigraphic controls on gold mineralization within the metavolcanic rocks of the Hoyle Pond Mine, Timmins. Econ Geol 103: 1341–1363

Ferenc Š, Rojkovič I (2001) Copper mineralization in the Permian basalts of the Hronicum Unit, Slovakia. Geolines 13: 22–27

Ferenc Š, Bakos F, Demko R, Koděra P (2014) Occurrences of siderite (Fe-carbonate) and quartz–sulphide mineralization near Lovinobaňa and Uderiná (Slovenské Rudohorie – Veporikum), Slovak Republic. Bull mineral.-petrolog Odd Nár Muz (Praha) 22: 25–41 (in Slovak)

García DR, Villanova-de-Benavent C, Butjosa L, Aiglsperger T, Melgarejo J C, Proenza JA, Iturralde-Vincent M, Garcia-Casco A (2015) Au mineralization in "listvenites" from Mina Descanso, Central Cuba: preliminary results. In: André-Meyer AS, Cathelineau M, Muchez P, Pirard E, Sindern S (eds) Mineral Resources in a Sustainable World. Vol. 1, Contributions from the 13th Biennial Meeting of the Society for Geology Applied to Mineral Deposits (SGA), 08/2015, Nancy (France), 197–200

Grecula P, Abonyi A, Abonyiová M, Antaš J, Bartalský B, Bartalský J, Dianiška I, Drnzík E, Ďuďa R, Gargulák M, Gazdačko Ľ, Hudáček J, Kobulský J, Lörinz L, Macko J, Návesňák D, Németh Z, Novotný L, Radvanec M, Rojkovič I, Rozložník L, Rozložník O, Varček C, Zlocha J (1995) Mineral raw deposits of Slovenské Rudohorie Mts., Vol. 1. Mineralia Slovaca Monograph, Bratislava, pp 1–834 (in Slovak)

Halls C, Zhao R (1995) Listvenite and related rocks: pespectives on terminology and mineralogy with reference to an occurrence at Cregganbaur, Mayo Co., Republic of Ireland. Miner Depos 30: 303–313

Hansen LD, Dipple GM, Gordon TM, Kellet DA (2005) Carbonated serpentinite (listwanite) at Atlin, British Columbia: a geological analogue to carbon dioxide sequestration. Canad Mineral 43: 225–239

Hovorka D (1965) Serpentinites of the Kohút Crystalline Complex and their metamorphic products. Acta Geol Geogr Univ Com, Geol 9: 91–140 (in Slovak)

Hovorka D (1978) Geochemistry of the West Carpathians Alpine-type Ultramafic Rocks. Náuka o Zemi, Geol 12. Veda, Bratislava, pp 1–153

Hovorka D, Ivan P, Jaroš J, Kratochvíl M, Reichwalder P, Rojkovič I, Spišiak J, Turanová L (1985) Ultramafic Rocks of the Western Carpathians, Czechoslovakia. Geological Institute of D. Štúr Press, Bratislava, pp 1–258

Hraško Ľ, Bakos F, Broska I, Demko R, Derco J, Ferenc Š, Fodorová V, Kováčik M, Kráľ J, Madarás J, Maglay J, Maťo Ľ, Nagy A, Németh Z, Putiš M, Radvanec M, Siman P, Šimon L, Tuček Ľ, Vozárová A, Zuberec J (2005) Assessment of Geological and Raw-Material Potential of the Slovenské Rudohorie – West Area and Possibilities of their Utilization for the Region Development. Unpublished report, State Geological Institute of D. Štúr, Bratislava, pp 1–139 (in Slovak)

Hurai V, Lexa O, Schulmann K, Montigny R, Prochaska W, Frank W, Konečný P, Kráľ J, Thomas R, Chovan M (2008) Mobilization of ore fluids during Alpine metamorphism: evidence from hydrothermal veins in the Variscan basement of Western Carpathians, Slovakia. Geofluids 8: 181–207

Ivan P (1984) Metasomatites (listvenites) replacing ultrabasics (Paleozoic, Inner Western Carpathians). Miner Slov 16: 103–114

Ivan P (1985) Hydrothermally–metasomatic alterations of ultrabasic rocks. In: Hovorka D (ed) Ultramafic Rocks of Western Carpathians, Czechoslovakia. Geological Institute of D. Štúr Press, Bratislava, pp 171–180

Ivan P, Hovorka D (1980) Co–Ni mineralization at Spišsko-gemerské Rudohorie Mts., suggestions for search. Geol Průzk 22: 225–228 (in Slovak)

Klein F, Bach W (2009) Fe–Ni–Co–O–S phase relations in peridotite–seawater interactions. J Petrol 50: 39–59

Klinec A (1976) Geological map of the Slovenské Rudohorie and Nízke Tatry Mountains, 1: 50 000. Geological Institute of D. Štúr, Bratislava

Kováčik M, Kráľ J, Maluski H (1996) Alpine metamorphic and thermochronological evolution of pre-Alpine metamorphic rocks in the South Veporic pre-Alpine metamorphic rocks. Miner Slov 28: 185–202 (in Slovak)

Maksimović Z, Pantó G (1982) Nickel-bearing phlogopite from the nickel–iron deposit Studena Voda (Macedonia). Bull Acad Serbe Sci Arts 80: 1–6

Maťo Ľ, Ferenc Š, Bakos F, Demko R, Kráľ J (2005) Ore Mineral Raw Materials of the Slovenské Rudohorie – West Area. In: Hraško Ľ (ed) Assessment of Geological and Raw-Material Potential of the Slovenské Rudohorie – West Area and Possibilities of their Utilization for the Region Development. Unpublished report, Geological Institute of D. Štúr, Bratislava, pp 1–317 (in Slovak)

Mikuš T, Spišiak J (2007) Chemical composition and alteration of Cr-spinels from Meliata and Penninic serpentinized peridotites (Western Carpathians and Eastern Alps). Geol Q 51: 257–270

Plašienka D, Grecula P, Putiš M, Hovorka D, Kováč M (1997) Evolution and structure of the Western Carpathians: an overview. In: Grecula P, Hovorka D, Putiš M (eds) Geological Evolution of the Western Carpathians. Mineralia Slovaca Monograph, Geocomplex and Geological Survey of Slovak Republic, Bratislava, pp 1–24

Plissart G, Féménias O, Maruntiu M, Diot H, Demaiffe D (2009) Mineralogy and geothermometry of gabbro-derived listvenites in the Tisovita-Iuti ophiolite, southwestern Romania. Canad Mineral 47: 81–105

Pouchou JL, Pichoir F (1985) "PAP" (φρZ) procedure for improved quantitative microanalysis. In: Armstrong JT (ed) Microbeam Analysis. San Francisco Press, San Francisco, pp 104–106

Rieder M, Cavazzini G, D'yakonov YS, Frank-Kamenetskii VA, Gottardi G, Guggenheim S, Kovaľ PV, Müller G, Neiva AMR, Radoslovich EW, Robert JL, Sassi FP, Takeda H, Weiss Z, Wones DR (1998) Nomenclature of the micas. Clay Clay Miner 46: 586–595

Rojkovič I (1985) Ore mineralization of ultramafic bodies of the Western Carpathians. Veda, Bratislava, pp 1–112 (in Slovak)

Sazonov VN (1975) Listvenitization and Ore Mineralization. Nauka, Moscow, pp 1–171 (in Russian)

Sazonov VN (1978) Chromium in Hydrothermal Process (on Example of the Ural Mts.). Nauka, Moscow, pp 1–286 (in Russian)

Shiga Y (1987) Behavior of iron, nickel, cobalt and sulfur during serpentinization, with reference to the Hayachine ultrabasic rocks of the Kamaishi mining district, northeastern Japan. Canad Mineral 25: 611–624

Simic V, Saric K, Miladinovic Z, Andric N, Vukovic N (2013) Listvenite from Serbia as gemstone resource. In: Schuster R (ed) 11th Workshop on Alpine Geological Studies & 7th European Symposium on Fossil Algae. Abstracts and Field Guides, 09/2013, Schladming. Berichte Geol B-A 99: 86

Slavkay M, Beňka J, Bezák V, Gargulák M, Hraško Ľ, Kováčik M, Petro M, Vozárová A, Hrušković S, Knésl J, Knéslová A, Kusein M, Maťová V, Tulis J (2004) Mineral deposits of the Slovenské Rudohorie Mts., Vol. 2. State Geological Institute of Dionýz Štúr, Bratislava, pp 1–286 (in Slovak)

Spišiak J, Pitoňák P, Caňo F (1994) Allanite and Al-chromite in corundum–phlogopite rocks from Jasenie–Kyslá area (Nízke Tatry Mountains). Miner Slov 26: 67–69 (in Slovak)

Styles MT, Sanna A, Lacinska AM, Naden J, Maroto-Valer M (2014) The variation in composition of ultramafic rocks and the effect on their suitability for carbon dioxide sequestration by mineralization following acid leaching. Greenhouse Gas Sci Technol 4, 440–451

Takasawa K, Sakae T, Takeyama H (1976) Nickeliferous fuchsite un the quartz–magnesite rocks from the Setogawa Group, Japan. Clay Sci 5: 57–65

Uher P, Ferenc Š, Spišiak J (2013) Cr–Ni muscovite from Muránska Zdychava near Revúca (Slovenské Rudohorie Mountains, central Slovakia). Bull mineral-petrolog Odd Nár Muz (Praha) 21: 62–66 (in Slovak)

Vass D, Began A, Gross P, Kahan Š, Köhler E, Lexa J, Nemčok J (1988) Regional geological classification of the Western Carpathians and northern offshoots of Pannonian Basin in Czechoslovakia area. Map, 1:500 000 scale. Slovak Geological Office and Geological Institute of D. Štúr, Bratislava

Vojtko R, Králiková S, Jeřábek P, Schuster R, Danišík M, Fügenschuch B, Minár J, Madarás J (2016) Geochronological evidence for Alpine tectono-thermal evolution of the Veporic Unit (Western Carpathians, Slovakia). Tectonophysics 666: 48–65